Thermochimica Acta, 129 (1988) 99–113
Elsevier Science Publishers B.V., Amsterdam – Printed in The Netherlands

ON THE THERMOCHEMISTRY OF THE RARE EARTH ANTIMONIDES. THE Dy–Sb SYSTEM

R. FERRO, G. BORZONE and G. CACCIAMANI

Istituto di Chimica Generale, Università di Genova, Viale Benedetto XV, 3 16132 Genova (Italy)

(Received 4 January 1988)

ABSTRACT

The data in the literature relevant to the rare earth antimonide phase diagrams and the crystallochemical and thermodynamic properties of the rare earth antimonides are summarized. The data obtained in an investigation of Dy–Sb compounds are reported. This investigation was performed using X-ray and metallographic analyses and calorimetric measurements of the heats of formation. The values of ΔH_{form} (kJ (g atom)$^{-1}$ ±2.0) for the following compounds were obtained for the reaction in the solid state at 300 K (the crystal structure data have also been confirmed): Dy_5Sb_3 (hP16-Mn_5Si_3-type), −105.5; Dy_4Sb_3 (cI28-anti-Th_3P_4-type), −111.5; DySb (cF8-NaCl-type), −114. These data, together with those relevant to the other rare earth antimonides, are discussed and their trends are in good agreement with the relationships proposed by Gschneidner. The experimental data are in agreement with those computed according to Miedema's model and, in the case of the rare-earth-rich alloys, also agree with those calculated according to Kubaschewski's suggestion based on the effective coordination numbers.

INTRODUCTION

The rare earths react with the pnicogens to form several compounds. These compounds are very useful when giving a systematic description of the binary compounds. The lanthanide pnictides generally have a very high thermal stability and high formation enthalpies (their bond mechanism may be considered to be intermediate between the metallic, covalent and possibly ionic types [1,2]).

It has often been stressed in the literature [3–5] that a systematic study of the various compounds formed by the different rare earths with given elements may be particularly useful for studying the effects of the progressive variation in the atomic parameters of the elements involved on the properties of the compounds.

Dedicated to Professor Oswald Kubaschewski in honour of his contribution to thermochemistry.

0040-6031/88/$03.50

An accurate measurement and assessment of the thermodynamic properties of the rare earth pnictides may therefore be very important, both as a contribution to general considerations (comparison between measured and computed data), and to a discussion on their alternative methods of preparation (direct synthesis by melting or sintering, through gas phase reaction, transport methods, etc.).

The assessment of the thermodynamic properties of these substances is also important because they have a promising future in the technological field (see, for instance, refs. 1 and 5 for reviews on various properties such as semiconducting, magnetic, electronic properties, etc.).

In previous papers we have reported the results obtained in the measurements of the heats of formation of arsenides [7], antimonides [8] and bismuthides [9] of rare earth metals. In this paper the data concerning the antimonides of La, Ce, Pr, Nd and Sm are reviewed and are compared with those which have just been obtained in the examination of the Dy–Sb system.

GENERAL INFORMATION ON THE ALLOYING BEHAVIOUR OF ANTIMONY WITH THE RARE EARTHS

Crystallochemistry of the rare earth antimonides

In the literature there is a wealth of detailed information on the crystal structures of the rare earth antimonides (see, for instance, refs. 1 and 10). Figure 1 is a summary of the various well-established R–Sb phases and their crystal structures. The close agreement which exists between the compounds formed by the "trivalent" rare earths is evident. There is a clear subdivision into two groups of systems: one group formed by the light rare earths and one group formed by the heavy rare earths (in agreement with their general behaviour, however, the formulae and structures of the compounds formed by Eu and Yb are quite different).

In Fig. 1, data have also been included for the heavy rare earth RSb_2 compounds, the stability of which has not been fully ascertained (metastable phases, high pressure phases?).

In the specific case of the Dy–Sb alloys which have just been investigated, the values of the lattice parameters measured are reported in Table 1 together with the values found in the literature.

Phase diagrams

Reliable phase diagram data are only available for a few R–Sb systems (the experimental determination of these data is very difficult owing to the very high melting temperatures, the high reactivity of the samples and the

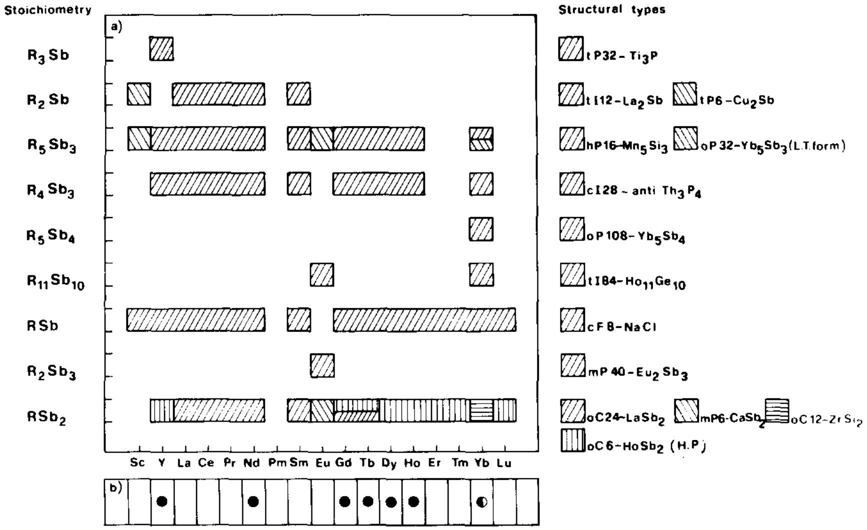

Fig. 1. The rare earth antimonides. (a) Phases and their crystal structures observed in the R–Sb systems. On the basis of DTA measurements the existence of other forms stable at high temperature has been suggested for the R_4Sb_3 compounds (R = Tb, Dy, Ho) and for the RSb compounds (R = Gd, Tb, Dy, Ho) [13,42,12,43]. Moreover, for many of the RSb compounds a variety of magnetic and structural phase transformations at low temperature have been described [17]. For $GdSb_2$ and $TbSb_2$ the $LaSb_2$-type structure has been reported only in a description of a high pressure investigation of the RSb_2 phases. For the heavy rare earth RSb_2 compounds another high pressure structure ($HoSb_2$-type) has been reported [20,21]. (b) Present state of the phase diagram investigation: ●, a complete recent determination is available; ◐, the phase diagram is only partially known.

high volatility of antimony. In Fig. 1 an indication is given of systems which have been, at least partially, investigated [12,13,42,43,51,52]. Figure 2 shows the phase diagram of the Dy–Sb system [12]. This can be considered as a reference for the heavy-rare-earth–antimony diagrams which have a similar shape. The phase diagrams formed by the light rare earths are a little more complex owing to the existence of another compound (R_2Sb). In all the systems the highest melting points are obtained for the congruent melting RSb compounds (all the other phases have a peritectic formation). In the Yb–Sb system, however, different behaviour has been observed: YbSb has a peritectic formation; Yb_4Sb_3 and $YbSb_2$ melt congruently [52].

Thermodynamics

As far as the thermodynamic properties of the rare earth antimonides are concerned, several investigations have been reported. Calorimetric measurements of the heat of formation have been carried out by us on different R–Sb systems: Y–Sb [22], La–Sb [23], Ce–Sb [24], Pr–Sb [25], Nd–Sb [26] and Sm–Sb [8].

Characteristics of rare earth monoantimonide powder evaporation have been studied by Viksman et al. [27] and subsequently assessed by Viksman and Gordienko [28]. Within the temperature range 1660–2360 K monoantimonides dissociate into atoms of rare earth and Sb. Standard values of the dissociation and formation enthalpies of La, Pr, Nd, Sm and Gd monoantimonides have been obtained.

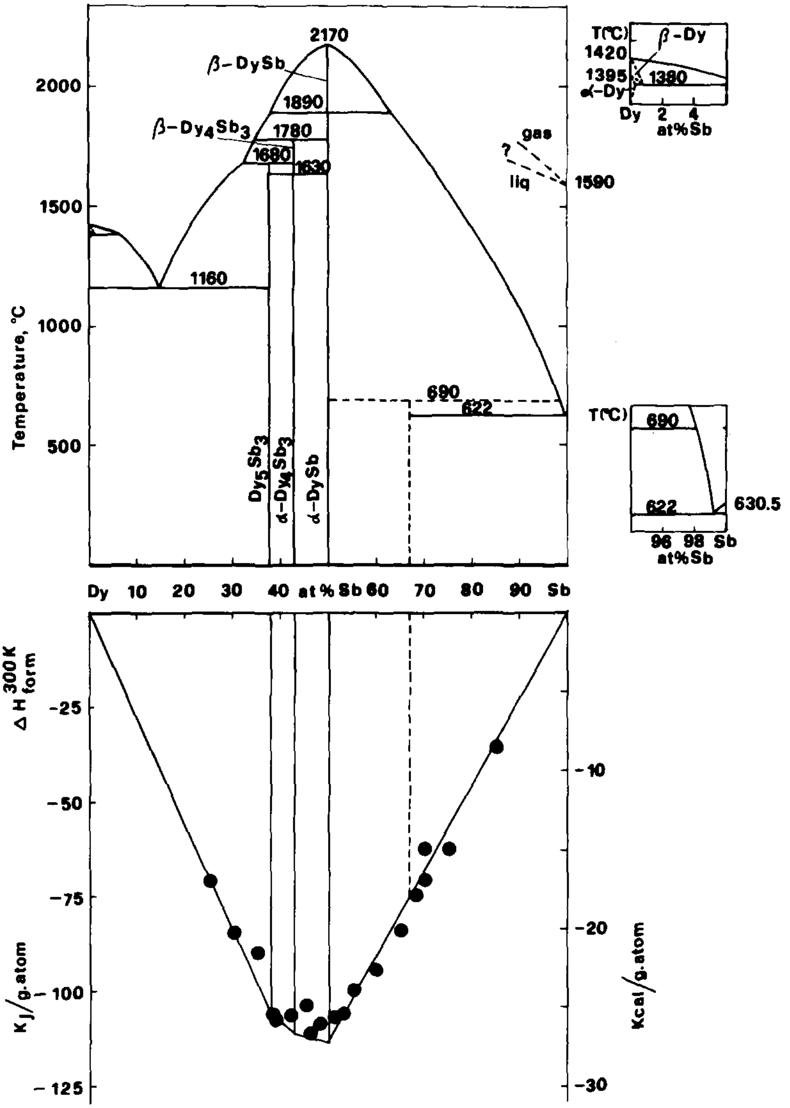

Fig. 2. Dy–Sb system. The trend in the heats of formation of the solid alloys is compared with the shape of the phase diagram (the parts relevant to the Dy- or Sb-rich alloys have been enlarged and reported on the right side). For the $DySb_2$ compound, whose formation is questionable, dotted lines are shown [13].

TABLE 1

Crystal structure data of Dy–Sb phases (room temperature if not otherwise stated)

Phase	Structural type	Unit cell dimensions (Å)			Reference
Dy_5Sb_3	Hexagonal	$a = 8.870$	$c = 6.266$	$c/a = 0.706_4$	11
	hP16-Mn_5Si_3	$a = 8.855$	$c = 6.244$	$c/a = 0.705$	12
		$a = 8.868$	$c = 6.263$	$c/a = 0.706$	13
		$a = 8.88_2$	$c = 6.27_0$	$c/a = 0.706$	This work
Dy_4Sb_3 [a]	Cubic				
	cI28-anti Th_3P_4	$a = 9.114$			14
		$a = 9.118$			12
		$a = 9.12$			15
		$a = 9.114$			This work
DySb [a]	Cubic	$a = 6.153$			16
	cF8-NaCl	$a = 6.157$			13
		$a = 6.155$			This work
		$a = 6.1316$ (presumably at 78 K)			17
	Tetragonal distortion of the NaCl type structure, low temperature form (11 K)	$a = 6.154$	$c = 6.113$		17,18
$DySb_2$ [b]	Orthorhombic oC6-$HoSb_2$, high temperature, high pressure form	$a = 3.273$	$b = 5.888$	$c = 7.965$	19,20,21

[a] The crystal structures of the high temperature forms of Dy_4Sb_3 and DySb are unknown.

[b] The unit cell parameters of $DySb_2$ (high temperature, high pressure form) have been obtained by Eatough and Hall [19]. The orientation of the crystallographic axes, however, is that suggested by Johnson [21].

Calorimetric and vapour pressure measurements on various monoantimonides have also been reported by Pratt and coworkers [29,30]. The congruent vaporization of CeSb was studied by Schiffman and Franzen [6] who measured the vapour pressure using a simultaneous weight-loss, mass-spectrometric Knudsen effusion technique.

Electromotive force measurements to obtain the heat, free energy and entropy of formation have been carried out on several antimonides of La [31,32], Gd [33] and Lu [34]. Partial and integral thermodynamic functions of dilute rare earth solutions in molten antimony have been obtained from e.m.f. measurements for several R–Sb systems (see, for instance, refs. 35 and 36).

EXPERIMENTAL

The metals employed were Dy and Sb with nominal purities of 99.9 and 99.99 wt%, respectively. A number of alloys of selected compositions were prepared by melting the metals in Ta crucibles (which were sealed by welding under argon). These alloys were prepared for use as reference alloys against those prepared in the calorimeter. A few crystallographic determinations were also carried out on these alloys. After annealing, the samples were subjected to the X-ray and metallographic examinations described below.

Calorimetric measurements

These were performed using a direct, isoperibolic, aneroid calorimeter, which has been fully described elsewhere [37]. Its construction was based on the building principles of an instrument described by Kubaschewski and Dench [38]. It consists of a thick aluminium cylinder containing two small furnaces. The furnaces are used to start the reaction in the sample and for the electric calibration. The sample consists of a mixture of the two elements, which were first reduced to fine powders (this operation was carried out under argon for Dy). These were then carefully mixed and compacted into an iron (or tantalum) crucible, which was subsequently sealed by electric welding under argon. The crucible was then inserted inside the small furnace of the calorimeter. After thermal equilibration the mixture was heated until the reaction started. The temperature of the calorimeter was followed by a multiple-junction thermopile (differentially connected to the similar thermopile of another calorimeter, identical to the first, used as a reference). The two calorimeters were symmetrically inserted in an aluminium block surrounded by a water ultrathermostat at $27 \pm 0.01°$C. The electric energy dissipated in the calorimeter in the reaction run was compared with that evolved in a number of calibration runs. The formation heats can be considered as having been measured at 300 K (thermostat temperature) because the sample inside the calorimeter cools down to this temperature during measurement.

The overall instrumental uncertainty was estimated to be ~ 1% [37,39]. The error of ± 2 kJ (g atom)$^{-1}$, generally ascribed to all measurements, is considered to include both this uncertainty and the effects due to small variations in composition or to possible quenching of disorder, etc. from a temperature higher than 300 K.

The complete range of composition was investigated and the different samples prepared in the calorimeter were subjected to a number of examinations, in order to check the composition and equilibrium state.

Metallographic examination

This was carried out (after dry polishing and etching in air or in dilute alcoholic HNO_3) on the largest sections of the specimens, in order to check the uniformity of composition, the phase distribution and the completion of the alloying reaction.

X-ray analysis

Powders of the various alloys were examined by the Debye method, using Fe $K\alpha$-radiation. Powder photographs were used both for phase analysis and identification and for lattice parameter measurements. These were carried out with least-squares fitting to the Nelson–Riley function. The observed diffraction intensities (visually scaled on the film) were compared with the calculated values obtained by means of a program prepared for the HP 9825 T calculator.

RESULTS

Crystal data

The results of the crystal lattice parameter measurements are reported in Table 1. The existence of the following phases was confirmed: Dy_5Sb_3, Dy_4Sb_3 and DySb compounds.

TABLE 2

Heats of formation of solid Dy–Sb alloys at 300 K, $(1-x)Dy + xSb \rightleftarrows Dy_{1-x}Sb_x$

Alloy number	Nominal composition x_{Sb}	Remarks	Diffraction lines observed in the powder photograph	ΔH_{form} (kJ (g atom)$^{-1}$ ± 2.0)
1	0.25	–	Mainly Dy_5Sb_3	−70.9
2	0.30	–	Mainly Dy_5Sb_3	−84.5
3	0.35	Not in equilibrium	DySb	(−90.0)
4	0.38	Nearly homogeneous	Dy_5Sb_3	−106.0
5	0.39	–	$Dy_5Sb_3 + Dy_4Sb_3$	−108.0
6	0.42	–	Dy_4Sb_3 + DySb	−106.5
7	0.45	Not in equilibrium	DySb	(−104.0)
8	0.46	–	Dy_4Sb_3 + DySb	−110.9
9	0.48	Non-uniform sample	DySb	(−108.8)
10	0.51	Non-uniform sample	Dy_4Sb_3 + DySb	−107.1
11	0.52_5	Nearly homogeneous	DySb	−106.4
12	0.55	Not far from homogeneity	DySb	−100.0
13	0.60	–	DySb	−94.5
14	0.65	–	DySb + X	−84.0
15	0.68	–	Mainly DySb + Sb	−74.6
16	0.70	–	Mainly DySb + Sb	−70.9
17	0.70	Incomplete reaction	Dy_4Sb_3 + mainly DySb	(−61.9)
18	0.75	Two phase	DySb + Sb	−62.5
19	0.85	–	DySb + Sb	−35.6

Interpolated values of ΔH_{form} for the various intermediate compounds in kJ (g atom)$^{-1}$ ± 2.0 (kcal (g atom)$^{-1}$ ± 0.5): Dy_5Sb_3, −105.5 (−25.2); Dy_4Sb_3, −111.5 (−26.6); DySb, −114 (−27.2). Near the $DySb_2$ composition, ΔH_{form} can be estimated as −76 kJ (g atom)$^{-1}$.

As far as the $DySb_2$ phase is concerned it must be remembered that no crystal data have been reported in the literature for the modification which is supposed to exist at room temperature and room pressure [13]. Data exist only for the high pressure form [19–21].

In this work, no clear indication of $DySb_2$ formation was obtained (either in the preparation of the reference samples or in the thermochemical experiments). Weak extra lines (in addition to those of DySb and Sb), which could not be indexed, were observed in a few samples near the 67 at% Sb composition.

Thermochemical data

The results obtained in the measurements of the formation heats are listed in Table 2. These values were used to trace the trend of the ΔH_{form} vs. composition curve (see Fig. 2) and to evaluate the most probable values of the ΔH of formation of the different compounds (also reported in Table 2). To carry out this evaluation, due consideration was also given to a few samples (reported in parentheses in Table 2) in which the equilibrium state was not completely achieved and whose reaction heats should therefore be considered to be a little lower than the correct values.

As pointed out by Wagner [40] and Kubaschewski et al. [41] further confirmation of the reliability of the ΔH values can be found in the relationship (see Fig. 2) between the ΔH trend and the melting behaviour of the different compositions. This point has already been discussed [8] and on that occasion the analogies between the phase diagrams and the ΔH/ composition diagrams of different R–Sb systems were stressed. The trend observed here for the dysprosium antimonides fits well with this general behaviour. Another check of the reliability of the values can be made through a comparison of the data reported by several researchers for the antimonides of different rare earths. Such a comparison is made for the

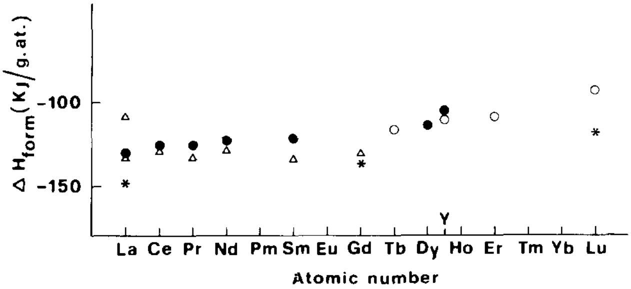

Fig. 3. ΔH_{form} values of the RSb compounds vs. the atomic number of the rare earth. ○ and ●, calorimetric data (● from our research group); △, vapour pressure measurements; *, e.m.f. measurements.

monoantimonides (that is the most exothermic compounds) in Table 3 and Fig. 3.

Calorimetric data, obtained by various workers, are available [29] for these compounds and values obtained indirectly (from vapour pressure measurements [6,8] or from e.m.f. methods [32,34]) are also known. The agreement between these values and those obtained through calorimetry can be considered to lie within the limits which can be expected in such a comparison. In the case of CeSb the excellent agreement between the calorimetric value and that recently obtained [6] using a very accurate vapour pressure technique, is particularly noteworthy.

DISCUSSION

Referring again to Table 3 and Fig. 3 and considering the present state of the calorimetric techniques, we would like to point out that the differences observed between a rare earth and its neighbours cannot be considered to be significant. The overall trend, however, certainly has a physical meaning and, in the case of the RSb phases, for instance, indicates a progressive decrease in the exothermic formation heats. A summary of such trends may therefore be useful.

It is well known [44,45] that a compact representation of all the equilibria existing in a set of R–X systems may be obtained using special "reduced parameters". The trends of these parameters, moreover, are well related to the trend of ΔH_{form}. With regard to this, Gschneidner [44] observed that the variations (as a function of the atomic number of R) in the cell volumes of specific rare earth compounds were due to the combined effect of the lanthanide contraction and of the volume variation accompanying the synthesis of the compound. He therefore suggested that a "relative volume ratio" could be useful. This can be calculated by firstly dividing the unit cell volume of the compound by the atomic volume of the rare earth metal involved. All these ratios are then normalized by dividing them by the ratio corresponding to one rare earth which is selected as a reference (in this paper we adopted lanthanum as our reference). An indication of the relative importance of the compound and of the elemental lanthanide contractions is given by the variations of these "relative volume ratios". If, for instance, the values increase along the rare earth sequence, the lanthanide contraction in the compounds is less marked and a decrease in the bond intensity and in the compound stability can be expected on going from La to Lu. This stability variation along the compound sequence can reasonably be correlated with the variation in the ΔH of formation. This is shown in Fig. 4.

It is also reasonable to expect a correlation between the formation heats, the volume ratios and the melting temperatures of the compounds of these elements which are similar to each other. This correlation is particularly

TABLE 3

Summary of the ΔH_{form} determinations for the RSb compounds (kJ (g atom)$^{-1}$)

Y	La	Ce	Pr	Nd	Sm	Gd	Tb	Dy	Er	Lu	Experimental method
−111 [29] −105 [22]	−131 [23]	−126 [24]	−126 [25]	−123 [26]	−122 [8]		−117 [30]	−114 [a]	−109 [30]	−93 [29]	Calorimetry
	−148 [32]					−137 [32]				−119 [34]	e.m.f. measurement
	−134 [28] −109 [30]	−129 [6]	−133 [28]	−129.5 [28]	−134.5 [28]	−131 [28]					Vapour pressure determination

[a] This work.

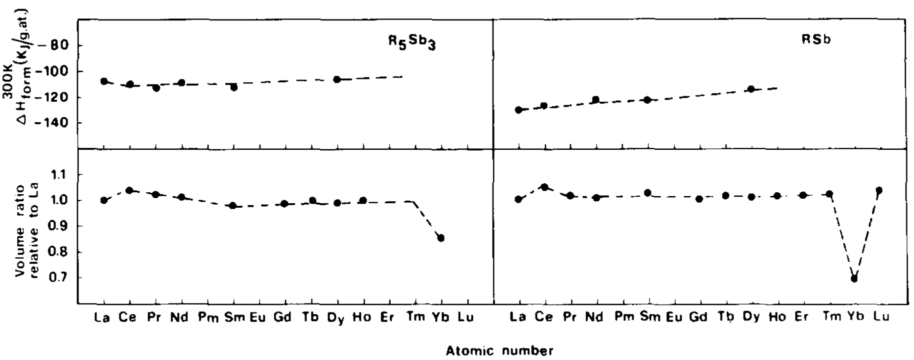

Fig. 4. Trends of ΔH_{form} of the R_5Sb_3 and RSb compounds in comparison with the trends of the "volume ratio" relative to La.

evident when the variation in "reduced melting temperatures" (melting temperature (K) of the phase divided by the melting temperature (K) of the rare earth involved) is discussed. These correlations have often been verified [46]. In our case, however, the agreement is not good. This may perhaps be because only a few melting data are available, and their determination is

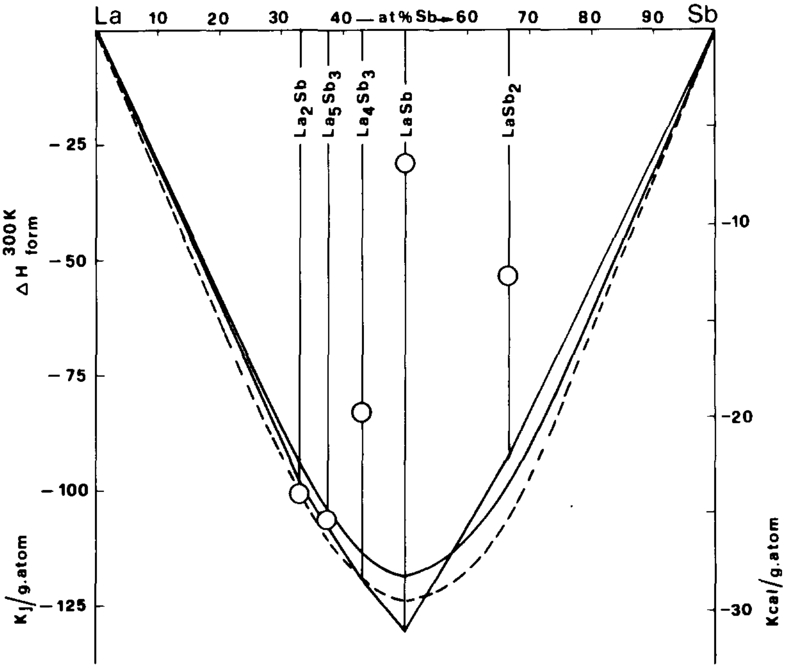

Fig. 5. ΔH_{form} for the La–Sb compounds. Comparison between experimental and calculated data. Polygonal continuous line, experimental data [23]; quasi-parabolic continuous line, computed according to Miedema's model [48]; dotted line, computed according to Colinet [49]; ○, Kubaschewski's intermetallic coordination term [50].

very difficult (very high melting points and very high reactivity and alteration of the samples at these temperatures).

In any case, from the trends shown in Figs. 3 and 4 it is possible to obtain the necessary values for the compounds for which no measurements are yet available by interpolation. (This is also important in view of the calculation and prediction of phase equilibria diagrams which can be drawn up by using computer programs such as that of Lukas et al. [47].)

In conclusion, it may be useful to compare the experimental data with those computed on the basis of a few different models. Such a comparison is made in Fig. 5 where all the data pertaining to the La–Sb system are reported (among the different rare earth antimonides those of lanthanum may be particularly interesting for this comparison, considering the high number of compounds which exist in this system).

As far as the computation of the formation heats is concerned, it is well known that Miedema has demonstrated that a good description of these data can be obtained by means of a cellular model. Consequently he suggested the following formula [48]

$$\Delta H_{\text{form}} = \frac{2\mathrm{f}(x)\left[(1-x)V_{\mathrm{A}}^{2/3} + xV_{\mathrm{B}}^{2/3}\right]}{\left(n_{\mathrm{WS,A}}\right)^{1/3} + \left(n_{\mathrm{WS,B}}\right)^{1/3}} \left\{-P(\Delta\phi^{\star})^2 + Q\left[(\Delta n_{\mathrm{WS}})^{1/3}\right]^2 - R\right\}$$

(for the alloy $\mathrm{A}_{1-x}\mathrm{B}_x$; $\Delta\phi^{\star} = \phi^{\star}_{\mathrm{A}} - \phi^{\star}_{\mathrm{B}}$; $\Delta n_{\mathrm{WS}} = n_{\mathrm{WS,A}} - n_{\mathrm{WS,B}}$) where V_{A} and V_{B} are the molar volumes of elements A and B in the alloy deduced from the molar volumes of pure A and B by means of the following expression

$$V_{\mathrm{A(alloy)}}^{2/3} = V_{\mathrm{A(pure\ A)}}^{2/3}\left[1 + ax(\phi^{\star}_{\mathrm{A}} - \phi^{\star}_{\mathrm{B}})\right]$$

($a = 0.07$ for trivalent metals and 0.04 for tetravalent or pentavalent metals). For an ordered alloy it is

$$\mathrm{f}(x) = c^{\mathrm{s}}_{\mathrm{A}} c^{\mathrm{s}}_{\mathrm{B}}\left[1 + 8(c^{\mathrm{s}}_{\mathrm{A}} c^{\mathrm{s}}_{\mathrm{B}})^2\right]$$

where $c^{\mathrm{s}}_{\mathrm{A}}$ represents the surface concentration, defined by

$$c^{\mathrm{s}}_{\mathrm{A}} = (1-x)V_{\mathrm{A}}^{2/3}\left[(1-x)V_{\mathrm{A}}^{2/3} + xV_{\mathrm{B}}^{2/3}\right]^{-1}$$

$\phi^{\star}_{\mathrm{A}}$ is the work function of the element A and Δn_{WS} is the electron density difference at the Wigner–Seitz atomic cell boundaries. Q is a constant and P and R are parameters depending on the type of elements involved.

The parameter values have been slightly adjusted by Colinet and Pasturel [49] who suggested that the difference in the enthalpies can be represented more correctly by assuming a variation in the hybridization term R along the series of lanthanides. The excellent agreement between the values computed according to these suggestions and the experimental values is shown in Fig. 5.

It should be noted, however, that the trends calculated from these formulae are continuous: the effect of the sharp change from the stoichiometry of one intermediate phase to another phase is not explicitly taken into account.

Note that a very simple model in which the structure of the phase involved is explicitly considered, has been proposed by Kubaschewski [50]. He proposed the following equation

$$-\Delta H_{\text{form}} = \frac{N_A L_A \left(C^{\star}_{A,\text{alloy}} - C^{\star}_{A,\text{metal}} \right)}{C^{\star}_{A,\text{metal}}} + \frac{N_B L_B \left(C^{\star}_{B,\text{alloy}} - C^{\star}_{B,\text{metal}} \right)}{C^{\star}_{B,\text{metal}}}$$

where N_A and N_B are the atomic fractions and L_A and L_B the sublimation heats of the metals involved. The heat of formation is related to the coordination increase and an "effective coordination number" $C^{\star}$ was defined in terms of the usual coordination numbers C using the following procedures

$$C^{\star}_A = \Sigma \frac{2r_A}{d_{AA}} C_A + \Sigma \frac{r_A + r_B}{d_{AB}} C_{AB}$$

for $d_{AA} < 2r_A$ and $d_{AB} < r_A + r_B$, and

$$C^{\star}_A = \Sigma \frac{\sqrt{2}\ 2r_A - d_{AA}}{(\sqrt{2} - 1)2r_A} C_A + \Sigma \frac{\sqrt{2}\,(r_A + r_B) - d_{AB}}{(\sqrt{2} - 1)(r_A + r_B)} C_{AB}$$

for $d_{AA} > 2r_A$ and $d_{AB} > r_A + r_B$

d are the interatomic distances and r the elementary radii.

Using the Kubaschewski formula the heats of formation of intermetallic phases can be correctly computed for a number of alloys in which the compound stabilities can be ascribed entirely to metallic bonds. Figure 5 shows the excellent agreement between the computed data and the experimental data for the rare-earth-rich compounds whose metallic character has already been pointed out [1,2]. The Kubaschewski coordination term, however, represents only a part of the overall formation heat in the Sb-rich compounds for which a more complex bond mechanism of intermediate ionic–covalent character has been found.

ACKNOWLEDGEMENT

The people of the Istituto di Chimica Generale of the Genoa University thank Dr. Kubaschewski for the extremely useful suggestions, advice and encouragement he has given them over the last 20 years. On the occasion of his 75th birthday, they would like to send him their congratulations and best wishes.

REFERENCES

1 F. Hulliger, in K.A. Gschneidner, Jr. and L. Eyring (Eds.), Handbook on the Physics and Chemistry of Rare Earths, Vol. IV, North-Holland, Amsterdam, 1979, p. 153.

2 F. Hulliger and H.R. Ott, J. Less-Common Met., 55 (1977) 103.

3 S.P. Yatsenko, A.A. Semyannikov, B.G. Semenov and K.A. Chuntonov, J. Less-Common Met., 64 (1979) 185.

4 K.A. Gschneidner, Jr. and F.W. Calderwood, Bull. Alloy Phase Diagrams, 4 (1983) 129.

5 K.A. Gschneidner, Jr. and O.D. McMasters, Monatsh. Chem., 102 (1971) 1499.

6 R.A. Schiffman and H.F. Franzen, High Temp. Sci., 15 (1982) 179.

7 G. Borzone, A. Borsese and R. Ferro, Gazz. Chim. Ital., 113 (1983) 235.

8 G. Borzone, A. Borsese, S. Delfino and R. Ferro, Z. Metallkd., 76 (1985) 208.

9 G. Borzone, A. Borsese and R. Ferro, Thermochim. Acta, 41 (1980) 175.

10 A. Iandelli and A. Palenzona, in K.A. Gschneidner, Jr. and L. Eyring (Eds.), Handbook on the Physics and Chemistry of the Rare Earths, Vol. II, North-Holland, Amsterdam, 1979, p. 1.

11 W. Rieger and E. Parthe, Acta Crystallogr. Sect. B, 24 (1968) 456.

12 K.E. Mironov, M.N. Abdusalyamova and O.R. Burnashev, Izv. Akad. Nauk SSSR, Neorg. Mater., 16 (1980) 1951.

13 M.N. Abdusalyamova, O.R. Burnashev and K.E. Mironov, J. Less-Common Met., 125 (1986) 1.

14 D. Hohnke and E. Parthe, Acta Crystallogr., 21 (1966) 435.

15 R.J. Gambino, J. Less-Common Met., 12 (1967) 344.

16 L.H. Brixner, J. Inorg. Nucl. Chem., 15 (1960) 199.

17 P.E. Holbourn and F.W.D. Woodhams, J. Solid State Chem., 38 (1981) 186.

18 F. Levy, Phys. Konden. Mater., 10 (1969) 85.

19 N.L. Eatough and H.T. Hall, Inorg. Chem., 8 (1969) 1439.

20 N.L. Eatough and H.T. Hall, Inorg. Chem., 9 (1970) 416.

21 Q. Johnson, Inorg. Chem., 10 (1971) 2089.

22 A. Borsese, G. Borzone, A. Saccone and R. Ferro, J. Less-Common Met., 52 (1977) 123.

23 G. Borzone, A. Borsese, A. Saccone and R. Ferro, J. Less-Common Met., 65 (1979) 253.

24 A. Borsese, G. Borzone, D. Mazzone and R. Ferro, J. Less-Common Met., 79 (1981) 57.

25 G. Borzone, A. Borsese, G. Zanicchi and R. Ferro, J. Therm. Anal., 25 (1982) 433.

26 A. Borsese, R. Ferro, R. Capelli and S. Delfino, J. Less-Common Met., 55 (1977) 77.

27 G.Sh. Viksman, S.P. Gordienko and M.N. Abdusalyamova, Poroshk. Metall., 12 (1980) 56; Chem. Abstr., 94 (1980) 36611e.

28 G.Sh. Viksman and G.P. Gordienko, Izv. Akad. Nauk SSSR, Neorg. Mater., 20 (1984) 1441.

29 K.S. Chua and J.N. Pratt, Thermochim. Acta, 8 (1974) 409.

30 J.N. Pratt and D.T. Underhill, unpublished work, University of Birmingham, 1972; quoted in ref. 9.

31 V.I. Goryacheva, A.V. Nikol'skaya and Ya.I. Gerasimov, Dokl. Akad. Nauk SSSR, 199 (1971) 632.

32 V.I. Goryacheva, A.V. Nikol'skaya and Ya.I. Gerasimov, Dokl. Akad. Nauk SSSR, 199 (1971) 380.

33 V.I. Goryacheva, N. Messauden, A.V. Nikol'skaya and Ya.I. Gerasimova, Vestn. Mosk. Univ., Ser. 2, Khim., 18 (1977) 749; Chem. Abstr., 88 (1978) 178021n.

34 Ya.I. Gerasimov, V.I. Goryacheva and V.P. Vasil'ev, Dokl. Akad. Nauk. SSSR, 247 (1979) 135; Chem. Abstr., 91 (1979) 146732r.

35 V.I. Kober, V.A. Dubinin, I.F. Nichkov and S.R. Kanevskii, Izv. Vyssh. Uchebn. Zaved., Tsvetn. Metall., 4 (1985) 108.

36 V.I. Kober, I.F. Nichkov, S.P. Raspopin and V.V. Shvydenko, Zh. Fiz. Khim., 60 (7) (1986) 1785.

37 R. Capelli, R. Ferro and A. Borsese, Thermochim. Acta, 10 (1974) 13.

38 O. Kubaschewski and W.A. Dench, Acta Metall., 3 (1955) 339.

39 R. Ferro, A. Borsese, R. Capelli and S. Delfino, Z. Anorg. Allg. Chem., 413 (1975) 279.

40 C. Wagner, Thermodynamics of Alloys, Addison–Wesley, Reading, MA, 1952, p. 83.

41 O. Kubaschewski, E.Ll. Evans and C.B. Alcock, Metallurgical Thermochemistry, Pergamon, London, 1967, p. 220.

42 M.N. Adbusalyamova, O.R. Burnashev and K.E. Mironov, J. Less-Common Met., 77 (1981) 81.

43 M.N. Abdusalyamova, O.R. Burnashev and K.E. Mironov, J. Less-Common Met., 102 (1984) 119.

44 K.A. Gschneidner, Jr., J. Less-Common Met., 17 (1969) 1.

45 K.A. Gschneidner, Jr. and F.W. Calderwood, Bull. Alloy Phase Diagrams, 7 (1986) 274.

46 S. Delfino, A. Saccone and R. Ferro, J. Less-Common Met., 102 (1984) 289.

47 H.L. Lukas, E.Th. Henig and B. Zimmermann, Calphad, 1 (1977) 225.

48 A.K. Niessen, F.R. de Boer, R. Boom, P.F. de Châtel, W.C.M. Mattens and A.R. Miedema, Calphad, 7 (1983) 51.

49 C. Colinet and A. Pasturel, J. Less-Common Met., 102 (1984) 239.

50 O. Kubaschewski, Proc. Symp. Physical Chemistry of Metal Solutions and Intermetallic Compounds, paper 3C. National Physics Laboratory, Teddington, 1958.

51 F.A. Schmidt and O.D. McMasters, J. Less-Common Met., 21 (1970) 415.

52 R.E. Bodnar and H. Steinfink, Inorg. Chem., 6 (1967) 327.

53 J.N. Pratt and K.S. Chua, Thermodynamic Studies of Some Rare Earth Alloys, Department of Physical Metallurgy and Science of Materials, University of Birmingham, June 1970.